Preparation, Characterization, and Some Properties of a T-Cage-Type S-Bridged $Rh^{III}{}_4Zn^{II}{}_3$ Heptanuclear Complex with a Defective $[Zn_3HO]^{5+}$ Core. Crystal Structure of Spontaneously Resolved $[\{Rh(aet)_3\}_4Zn_3HO]Br_5$ (aet=2-Aminoethanethiolate)

Takumi KONNO,* Ken-ichi OKAMOTO, and Jinsai HIDAKA
Department of Chemistry, University of Tsukuba, Tsukuba, Ibaraki 305

(Received June 21, 1993)

The reaction of *fac*(*S*)-$[Rh(aet)_3]$ with $ZnBr_2$ in water produced a T-cage-type S-bridged polynuclear complex with a "defective" $[Zn_3HO]^{5+}$ core, $[\{Rh(aet)_3\}_4Zn_3HO]Br_5$ (**1**Br_5), which was subject to spontaneous resolution to give $(+)^{CD}_{350}$ and $(-)^{CD}_{350}$ isomers. **1** was also optically resolved into the two isomers with use of $[Sb_2(R,R\text{-tartrate})_2]^{2-}$. The crystal structure and absolute configuration for the spontaneously resolved $(-)^{CD}_{350}$ isomer were determined by X-ray crystallography. $[\{Rh(C_2H_6NS)_3\}_4Zn_3HO]Br_5\cdot 9H_2O$, crystallizes in the cubic space group $P2_13$ with $a=19.186$ (1) Å, $V=7062.1$ (4) $Å^3$, $Z=4$, and $R=0.0648$. In **1** the four octahedral *fac*(*S*)-$[Rh(aet)_3]$ subunits are bound to a quasi-tetrahedral $[Zn_3HO]^{5+}$ core in a tetrahedral arrangement. The chiral configurations are regulated to Δ for all *fac*(*S*)-$[Rh(aet)_3]$ subunits and *R* for all asymmetric bridging sulfur atoms in $(-)^{CD}_{350}$-**1**, giving a quasi-T symmetrical structure. **1** is unstable in water and convertible to a T-cage-type octanuclear complex with a "complete" $[Zn_4O]^{6+}$ core, $[\{Rh(aet)_3\}_4Zn_4O]^{6+}$ (**2**), and to a linear-type S-bridged trinuclear complex, $[Co\{Rh(aet)_3\}_2]^{3+}$, by adding $ZnBr_2$ and $[CoCl(NH_3)_5]Cl_2$, respectively. The electronic absorption and circular dichroism (CD) spectral behavior of **1** are discussed in comparison with those of **2**.

There has been considerable research interest in the stereochemistry of S-bridged polynuclear complexes with 2-aminoethanethiolate (aet; $NH_2CH_2CH_2S^-$) or L-cysteinate (L-cys; $NH_2CH(COO^-)CH_2S^-$) over the past three decades.[1—25] The S-bridged polynuclear complexes composed of chiral *fac*(*S*)-[M(aet or L-cys-*N*,*S*)$_3$]$^{0 \text{ or } 3-}$ (M = Co(III), Rh(III), or Ir(III)) subunits[5—25] are of special interest in virtue of the optical isomerism. The initial investigations of this class complexes were carried out by Busch et al., who prepared linear-type S-bridged trinuclear complexes, $[M'\{Co(aet)_3\}_2]^{2+ \text{ or } 3+}$ (M′ = Ni(II) or Co(III)), by reacting fac(S)-$[Co(aet)_3]$ with Ni^{2+} or $[CoBr(NH_3)_5]^{2+}$.[5] The linear-type trinuclear structure has been confirmed by the separation and resolution of the meso ($\Delta\Lambda$) and optical active ($\Delta\Delta$ and $\Lambda\Lambda$) isomers for M′ = Co(III),[6] and recently determined by single crystal X-ray analyses for M′ = Co(III)[10] and Ni(II).[23] The investigations of the linear-type S-bridged trinuclear complexes have been extended to include Fe(III), Ru(III), or Os(III) at the center[7,11] and *fac*(*S*)-[Co(L-cys-*N*,*S*)$_3$]$^{3-}$,[12—15] *fac*(*S*)-[Rh(aet or L-cys-*N*,*S*)$_3$]$^{0 \text{ or } 3-}$,[16] or *fac*(*S*)-[Ir(aet or L-cys-*N*,*S*)$_3$]$^{0 \text{ or } 3-}$[24] in the terminal of the trinuclear structure. These results demonstrated that *fac*(*S*)-[M(aet or L-cys-*N*,*S*)$_3$]$^{0 \text{ or } 3-}$ function as a terdentate ligand to metal ions which prefer to take an octahedral coordination geometry. While these mononuclear complexes have been recognized to react also with metal ions such as Zn^{2+} and Cd^{2+},[6,8—10] which prefer to take a tetrahedral geometry, the stereochemistry of the S-bridged complexes containing these metal ions has long been remained largely unexplored, although the reaction products from *fac*(*S*)-$[Co(aet)_3]$ and Zn^{2+} or Cd^{2+} have been assumed to be linear-type S-bridged trinuclear or tetranuclear complexes.[6,8,9]

We have recently found that the reaction of *fac*(*S*)-$[Co(aet)_3]$ with Zn^{2+} in water does not give a proposed linear-type complex but a novel T-cage-type octanuclear complex with a "complete" $[Zn_4O]^{6+}$ core, $[\{Co(aet)_3\}_4Zn_4O]^{6+}$,[20] and that the linear-type trinuclear complexes, $[Co\{M(aet)_3\}_2]^{3+}$ (M=Rh(III) or Ir(III)), are convertible to T-cage-type octanuclear complexes with a "complete" $[Zn_xCo_{4-x}]^{6+}$ core, $[\{M(aet)_3\}_4Zn_xCo_{4-x}O]^{6+}$, by the reactions with Zn powder in water.[19,25] These T-cage-type octanuclear complexes with a "complete" core are fairly stable in solution and exhibited unique stereochemical and spectrochemical behavior which have not been observed for the related linear-type trinuclear complexes. Furthermore, in a preliminary report[18] we have pointed out that a T-cage-type S-bridged heptanuclear complex with a "defective" core, which contains four *fac*(*S*)-$[Rh(aet)_3]$ subunits and three zinc atoms, is readily formed from *fac*(*S*)-$[Rh(aet)_3]$ and Zn^{2+} at room temperature in water. The T-cage-type $Rh^{III}{}_4Zn^{II}{}_3$ complex with a "defective" core is unstable in solution and may be considered as a precursor of the stable T-cage-type $Rh^{III}{}_4Zn^{II}{}_4$ complex with a "complete" core. It is anticipated that detailed investigations of the structure and properties of the T-cage-type Rh_4Zn_3 complex with a "defective" core will contribute significantly to our understanding of the chemistry of the T-cage-type S-bridged polynuclear complexes. In this paper we report on the detailed study of the T-cage-type S-bridged $Rh^{III}{}_4Zn^{II}{}_3$ complex with a "defective" core, which is characterized as $[\{Rh(aet)_3\}_4Zn_3HO]^{5+}$ (Fig. 1), rather than $[\{Rh(aet)_3\}_4Zn_3O]^{4+}$,[18] by a combination of X-ray diffraction, plasma emission spectral and elemental

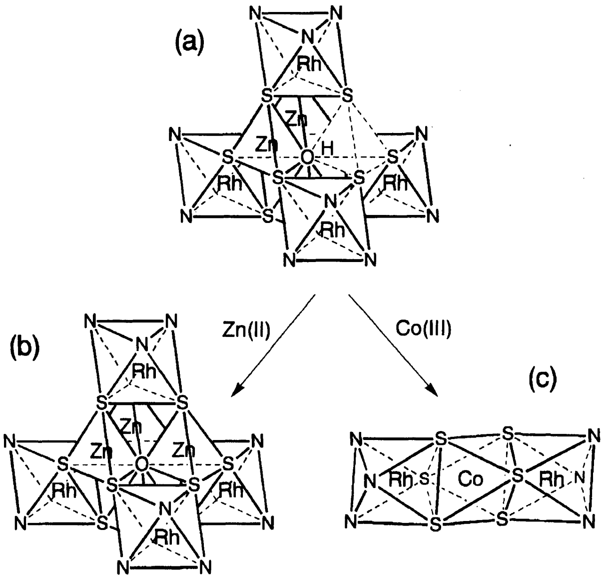

Fig. 1. Polyhedral representations of $[\{Rh(aet)_3\}_4Zn_3HO]^{5+}$ (a), $[\{Rh(aet)_3\}_4Zn_4O]^{6+}$ (b), and $[Co\{Rh(aet)_3\}_2]^{3+}$ (c).

analyses, molar conductivity, and absorption, CD, and ^{1}H NMR spectra.

Experimental

Preparation of $[\{Rh(aet)_3\}_4Zn_3HO]^{5+}$ (1). To a suspension (pH=ca. 7) containing 0.5 g (1.5 mmol) of *fac*(*S*)-$[Rh(aet)_3]$[26] in 25 cm^3 of water was added a solution (pH=ca. 7) containing 0.5 g (2.2 mmol) of $ZnBr_2$ in 2.5 cm^3 of water. The mixture was stirred at room temperature for 30 min, whereupon the suspension became a clear orange-yellow solution (pH=ca. 3). To this was added 5 g of NaBr or NH_4Br in 20 cm^3 of water, followed by storing in a refrigerator overnight. The resulting yellow-orange complex ($\mathbf{1}Br_5 \cdot 9H_2O \cdot 0.8ZnBr_2$) was collected by filtration and then washed with methanol. This complex was also prepared using $ZnCl_2$, $ZnSO_4 \cdot 7H_2O$, or $Zn(NO_3)_2 \cdot 6H_2O$ instead of $ZnBr_2$. Yield; 0.66 g (77%). Anal. Calcd for $[\{Rh(C_2H_6NS)_3\}_4Zn_3HO]Br_5 \cdot 9H_2O \cdot 0.8ZnBr_2$: C, 12.64; H, 4.02; N, 7.37; Zn, 10.90; Rh, 18.05%. Found: C, 12.81; H, 4.14; N, 7.37; Zn, 11.15; Rh, 18.21%.

The nitrate salt of **1** was obtained by the addition of an aqueous solution (4 cm^3) of $NaNO_3$ (2 g) to an aqueous solution (4 cm^3) of $\mathbf{1} \cdot 9H_2O \cdot 0.8ZnBr_2$ (0.2 g), followed by cooling in a refrigerator for several hours. Anal. Calcd for $[\{Rh(C_2H_6NS)_3\}_4Zn_3HO](NO_3)_5 \cdot 2H_2O$: C, 15.30; H, 4.12; N, 12.63; Zn, 10.41; Rh, 21.84%. Found: C, 15.27; H, 4.12; N, 12.63; Zn, 10.04; Rh, 21.84%.

Recrystallization of $\mathbf{1}Br_5 \cdot 9H_2O \cdot 0.8ZnBr_2$ from water in a refrigerator afforded spontaneously resolved yellow-orange crystals; each crystal that was picked up from the bulk showed a positive or a negative CD sign with the same $|\Delta\varepsilon|$ value at the same wavelength. One of the yellow-orange crystals ($\mathbf{1}Br_5 \cdot 9H_2O$), which showed a negative CD value at 350 nm, was used for X-ray analysis. Anal. Calcd for $[\{Rh(C_2H_6NS)_4Zn_3HO]Br_5 \cdot 9H_2O$: C, 13.73; H, 4.37; N, 8.00; Zn, 9.34; Rh, 19.60%. Found: C, 13.43; H, 4.33; N, 7.70; Zn, 9.27; Rh, 19.48%.

Slow evaporation of an aqueous solution containing $\mathbf{1}Br_5 \cdot 9H_2O \cdot 0.8ZnBr_2$ (0.2 g) and $ZnBr_2$ (0.05 g) at room temperature gave spontaneously resolved yellow crystals. The absorption and CD spectra of this yellow complex were identical with that of $[\{Rh(aet)_3\}_4Zn_4O]Br_6$ ($\mathbf{2}Br_6$), which can be prepared directly by the reaction of *fac*(*S*)-$[Rh(aet)_3]$ with a mixture of $ZnBr_2$ and ZnO in water at room temperature.[25] Slow evaporation of an aqueous solution of $\mathbf{1}Br_5 \cdot 9H_2O \cdot 0.8ZnBr_2$ at room temperature resulted in the formation of spontaneously resolved orange-yellow crystals of a mixture of $\mathbf{1}Br_5$ and $\mathbf{2}Br_6$.

Optical Resolution of $[\{Rh(aet)_3\}_4Zn_3HO]^{5+}$ (1). To a solution containing 0.5 g (0.2 mmol) of $\mathbf{1} \cdot 9H_2O \cdot 0.8ZnBr_2$ in 50 cm^3 of water was added a solution containing 2.5 g (3.7 mmol) of $K_2[Sb_2(R,R\text{-tartrate})_2] \cdot 3H_2O$ in 50 cm^3 of water. The mixture was allowed to stand at room temperature for 20 min and the resulting yellow needle microcrystals, which showed a negative CD value at 350 nm ($(-)^{CD}_{350}$ diastereomer), were collected by filtration.

The yellow filtrate, which showed a positive CD value at 350 nm, was stored in a refrigerator overnight and the resulting white-yellow powder was filtered off. This filtrate was concentrated to dryness and then the yellow residue was dissolved in 10 cm^3 of water. To this was added 5 cm^3 of a saturated $NaNO_3$ aqueous solution, followed by storing in a refrigerator for one day. The resulting orange-yellow needle crystals ($(+)^{CD}_{350}$-$\mathbf{1}(NO_3)_5 \cdot 2H_2O$) were collected by filtration.

To a suspension containing 0.2 g of the $(-)^{CD}_{350}$ diastereomer in 4 cm^3 of water was added 2 g of $NaNO_3$ in 4 cm^3 of water. The mixture was stirred at room temperature for 10 min, followed by cooling in a refrigerator for 2 h. The resulting orange-yellow complex ($(-)^{CD}_{350}$-$\mathbf{1}(NO_3)_5 \cdot 2H_2O$) was collected by filtration and recrystallized from water by adding a few drops of a saturated $NaNO_3$ aqueous solution. Anal. Calcd for $[\{Rh(C_2H_6NS)_3\}_4Zn_3HO](NO_3)_5 \cdot 2H_2O$: C, 15.30; H, 4.12; N, 12.63; Zn, 10.41; Rh, 21.84%. Found for $(+)^{CD}_{350}$ isomer: C, 15.15; H, 4.05; N, 12.70; Zn, 10.15; Rh, 21.51%. Found for $(-)^{CD}_{350}$ isomer: C, 15.56; H, 3.99; N, 12.75; Zn, 10.33; Rh, 22.20%. Visible-UV spectrum, H_2O solvent [σ_{max}, 10^3 cm^{-1} ($\log\varepsilon$; ε in mol^{-1} dm^3 cm^{-1})]: 23.7 (2.95 sh), 28.2 (3.35 sh), 31.8 (3.62 sh), 46.08 (5.14). The sh label denotes a shoulder. CD spectrum for the $(-)^{CD}_{350}$ isomer, H_2O solvent [σ_{max}, 10^3 cm^{-1} ($\Delta\varepsilon$; ε in mol^{-1} dm^3 cm^{-1})]: 27.70 (−32.7), 34.60 (−4.9), 37.59 (+12.1), 42.74 (−78.4), 47.85 (+218.8).

The absorption and CD spectra of $(+)^{CD}_{350}$- and $(-)^{CD}_{350}$-$\mathbf{1}(NO_3)_5$ were almost identical with those of spontaneously resolved $(+)^{CD}_{350}$- and $(-)^{CD}_{350}$-$\mathbf{1}Br_5$, respectively.

Reaction of $[\{Rh(aet)_3\}_4Zn_3HO]^{5+}$ (1) with $[CoCl(NH_3)_5]^{2+}$. To a solution containing 0.1 g (0.05 mmol) of $(-)^{CD}_{350}$-$\mathbf{1}(NO_3)_5 \cdot 2H_2O$ in 4 cm^3 of water was added 0.05 g (0.2 mmol) of $[CoCl(NH_3)_5]Cl_2$. The mixture was stirred at 50 °C for 1 h, whereupon the solution color turned from orange-yellow to deep dark brown. It was found from the SP-Sephadex C-25 column chromatography (Na$^+$ form) that the resulting dark brown solution contained $\Delta\Delta$-$[Co\{Rh(aet)_3\}_2]^{3+}$[16] and $\Delta\Delta\Delta\Delta$-$[\{Rh(aet)_3\}_4Zn_4O]^{6+}$[25] in a ratio of ca. 2 : 3.

Measurements. The electronic absorption spectra were recorded with a JASCO UVIDEC-505 or UVIDEC-610C spectrophotometer, and the CD spectra with a JASCO J-600 spectropolarimeter. The concentrations of Rh and Zn in the complexes were determined with a Nippon Jarrel-Ash ICPA-575 ICP spectrophotometer. The ^1H NMR spectra were recorded with a BRUKER AM-500 NMR spectrometer at the probe temperature in D_2O. Sodium 4,4-dimethyl-4-silapentane-1-sulfonate (DSS) was used as the internal reference. The molar conductivities were measured with a Horiba DS-14 conductivity meter at 22 °C in water.

X-Ray Structure Determination. Single-crystal X-ray diffraction experiments were performed on an Enraf Nonius CAD4 diffractometer with a graphite-monochromatized Mo $K\alpha$ radiation. Unit cell parameters were determined by a least-squares refinement, using the setting angles of 25 reflections in the range $15<2\theta<17°$. The systematic absences led to the choice of either the space group $P2_12_12_1$ (No. 19) or $P2_13$ (No. 198). When the structure was solved by using the space group $P2_12_12_1$, all atoms of the complex cation exist almost on the positions expected for the site symmetry of $P2_13$. Hence, the space group was deduced to be $P2_13$, and this assignment was confirmed by the eventual structure refinement. Crystallographic data are summarized in Table 1. The intensity data were collected by the ω–2θ scan mode up to $2\theta=50°$. A total of 6824 reflections were collected, 1691 of which were considered as "observed" ($F_o>5\sigma(F_o)$). Data reduction and application of Lorentz, polarization, decomposition, and empirical absorption corrections based on a series of ψ scans were carried out by using the Enraf Nonius Structure Determination Package.[27)]

The structure for the space group $P2_12_12_1$ was solved by direct method[27)] and conventional difference Fourier techniques. The structure for the space group $P2_13$ was solved by using the non-hydrogen atom positions of one-third of the formula unit obtained from the space group $P2_12_12_1$ and was refined by full-matrix least-squares techniques using SHELX76.[28)] All non-hydrogen atoms were refined anisotropically and hydrogen atoms were not included in the calculation. Scattering factors and anomalous dispersion corrections for Rh and Zn were taken from Ref. 29, while all others were supplied in SHELX76. The RhB, ZnB, and O atoms in the complex cation and four Br atoms (Br2, Br3, Br4A, Br4B) were constrained to the special positions of symmetry 3. Refining the site occupancy factors of Zn and Br atoms yielded values of ZnA=0.79, ZnB=0.26, Br1=0.68, Br2=0.12, Br3=0.33, Br4A=0.15, and Br4B=0.15, and these atoms were refined with site occupancy factors of ZnA=0.75, ZnB=0.25. Br1=0.85, Br2=0.15, Br3=1/3, Br4A=1/6, and Br4B=1/6. The final difference Fourier map showed several peaks in the range 1.0—1.3 e Å^{-3}, all in the vicinity of Br1 and Br2. Non-hydrogen atom coordinates are listed in Table 2.[30)]

Table 1. Crystallographic Data for $(-)^{CD}_{350}$-[{Rh(aet)$_3$}$_4$Zn$_3$HO]Br$_5$·9H$_2$O ($(-)^{CD}_{350}$-**1**Br$_5$·9H$_2$O)

Formula	$C_{24}H_{91}N_{12}O_{10}S_{12}Zn_3Br_5Rh_4$
F.W.	2100.2
Cryst system	Cubic
Space group	$P2_13$ (No. 198)
a/Å	19.186(1)
V/Å^3	7062.1(4)
Z	4
D_{calcd}/g cm^{-3}	1.98
Cryst dimens/mm	0.12×0.12×0.24
μ/cm^{-1}	49.5
Transm coeff	0.968—1.000
Temp/K	296
λ(Mo $K\alpha$)/Å	0.71073
$R^{a)}$	0.0648
$R_w{}^{b,c)}$	0.0645
$R'^{a,e)}$	0.0711
$R'_w{}^{b,d,e)}$	0.0711
$R'/R^{f)}$	1.10

a) $R=\Sigma|(|F_o|-|F_c|)|/\Sigma(|F_o|)$.
b) $R_w=(\Sigma_w(|F_o|-|F_c|)^2/\Sigma_w(|F_o|)^2)^{1/2}$.
c) $w=2.75/(\sigma^2(F_o+(1.7\times10^{-3})|F_o|^2)$.
d) $w=2.98/(\sigma^2(F_o+(1.7\times10^{-3})|F_o|^2)$. e) Refinement in the enantiomeric parameters. f) Hamilton test;[32)] $R_{1,1500—2000,0.005}=1.0026—1.0020$.

Results and Discussion

Crystal Structure and Characterization of $(-)^{CD}_{350}$-[{Rh(aet)$_3$}$_4$Zn$_3$HO]Br$_5$ ($(-)^{CD}_{350}$-1Br$_5$). A perspective drawing of the entire complex cation $(-)^{CD}_{350}$-**1**, which has a crystallographically imposed C_3 axis through the RhB, O, and ZnB atoms, is given in Fig. 2. The selected bond lengths and angles are listed

Table 2. Final Atomic Coordinates, Equivalent Isotropic Thermal Parameters (B_{eq}/Å^2),[a)] and Occupancy Factors (*occ*)

Atom	*x*	*y*	*z*	B_{eq}	*occ*
RhA	0.0682(1)	0.1438(1)	0.8677(1)	3.40(7)	
S1A	0.1684(3)	0.1449(3)	0.9365(3)	4.01(23)	
S2A	−0.0051(3)	0.1881(3)	0.9535(3)	3.67(22)	
S3A	0.0417(3)	0.0281(3)	0.8919(3)	4.06(23)	
N1A	−0.0198(10)	0.1412(10)	0.8013(9)	4.87(88)	
N2A	0.1359(9)	0.1096(10)	0.7876(8)	4.93(88)	
N3A	0.0886(12)	0.2483(10)	0.8431(10)	6.0 (11)	
C1A	0.2276(14)	0.1033(24)	0.8778(12)	8.2 (19)	
C2A	0.2054(21)	0.0979(36)	0.8199(39)	20.7 (51)	
C3A	0.0135(13)	0.2814(10)	0.9419(11)	4.7 (10)	
C4A	0.0834(15)	0.2921(11)	0.9077(13)	5.7 (13)	
C5A	−0.0453(19)	0.0172(18)	0.8458(14)	8.6 (19)	
C6A	−0.0400(19)	0.0680(18)	0.7863(19)	10.7 (22)	
RhB	0.1913(1)	0.1913(1)	0.1913(1)	2.88(5)	1/3
S1B	0.2383(3)	0.1039(3)	1.1212(3)	3.56(22)	
N1B	0.2525(11)	0.1535(9)	1.2741(9)	4.98(92)	
C1B	0.3070(14)	0.1565(18)	1.0752(17)	8.0 (17)	
C2B	0.2179(18)	0.1016(24)	1.3166(20)	10.8 (24)	
ZnA	0.1647(1)	0.0676(1)	1.0312(1)	2.65(11)	0.75
ZnB	0.0083(1)	0.0083(1)	0.0083(1)	3.03(9)	0.25
O	0.0682(6)	0.0682(6)	0.0682(6)	2.71(34)	1/3
Br1	0.4326(5)	0.1947(5)	0.2544(4)	17.93(59)	0.85
Br2	0.3177(7)	0.3177(7)	0.3177(7)	16.50(89)	0.15
Br3	−0.0718(2)	0.4282(2)	0.0718(2)	6.69(13)	1/3
Br4A	−0.2638(5)	0.2362(5)	0.2638(5)	7.80(34)	1/6
Br4B	−0.2907(4)	0.2093(4)	0.2907(4)	8.71(55)	1/6
O1W	0.8253(24)	0.1488(15)	0.4472(16)	20.0 (28)	
O2W	−0.3861(16)	0.5425(19)	0.2740(16)	16.3 (25)	
O3W	0.4017(16)	0.5492(19)	0.5271(16)	15.1 (23)	

a) B_{eq} is the arithmetic mean of the principal axes of the thermal ellipsoid.

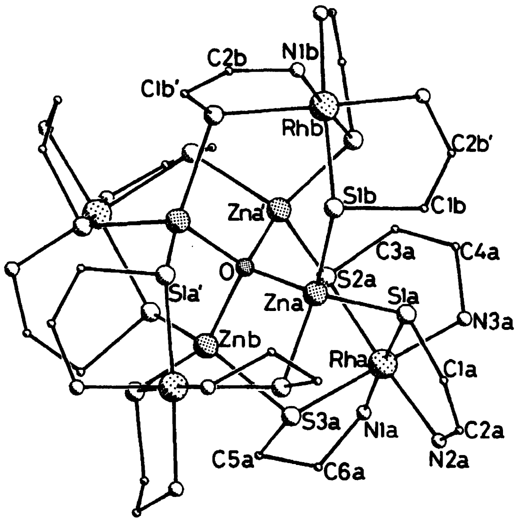

Fig. 2. Perspective view of $(-)^{\mathrm{CD}}_{350}$-**1** with the atomic labeling scheme.

Table 3. Selected Bond Distances (Å) and Angles (deg.)

RhA–S1A	2.331(5)	S2A–ZnA	2.341(6)
RhA–S2A	2.327(5)	S3A–ZnB	2.355(6)
RhA–S3A	2.325(6)	RhB–S1B	2.332(5)
RhA–N1A	2.115(18)	RhB–N1B	2.105(18)
RhA–N2A	2.115(15)	S1B–ZnA	2.337(6)
RhA–N3A	2.096(18)	ZnA–O	1.983(7)
S1A–ZnA	2.345(6)	ZnB–O	1.990(20)
S1A–RhA–S2A	95.4(2)	N2A–RhA–N3A	91.1(8)
S1A–RhA–S3A	94.3(2)	S1B–RhB–S1B	95.0(2)
S2A–RhA–S3A	94.3(2)	S1B–RhB–N1B	88.4(5)
S1A–RhA–N1A	177.4(5)	N1B–RhB–N1B	91.8(6)
S2A–RhA–N1A	87.2(5)	S1A–ZnA–S2A	110.8(2)
S3A–RhA–N1A	85.6(5)	S1A–ZnA–S1B	111.4(2)
S1A–RhA–N2A	84.8(6)	S2A–ZnA–S1B	112.5(2)
S2A–RhA–N2A	176.6(5)	S3A–ZnB–S3A	111.5(1)
S3A–RhA–N2A	89.0(5)	S1A–ZnA–O	107.6(2)
S1A–RhA–N3A	88.0(6)	S2A–ZnA–O	107.0(4)
S2A–RhA–N3A	85.5(6)	S1B–ZnA–O	107.3(5)
S3A–RhA–N3A	177.6(6)	S3A–ZnB–O	107.3(2)
N1A–RhA–N2A	92.6(7)	ZnA–O–ZnA	109.8(5)
N1A–RhA–N3A	92.1(8)	ZnA–O–ZnB	109.2(5)

in Table 3.

The entire complex cation **1** appears to consist of four approximately octahedral *fac*(*S*)-[Rh(aet)$_3$] subunits, four Zn atoms, and one central O atom. However, refining the occupancy factors of ZnA and ZnB yielded the values of 0.79 and 0.26, respectively, and the plasma emission spectral analysis gave the value of Rh : Zn = 4 : 3.00. These results indicate that **1** actually contains three Zn atoms, which are distributed in four locations with a site occupancy of 3/4. The Br anions are highly disordered (Table 2), and therefore, the charge of the complex cation **1** can not be determined directly from the X-ray analysis, although refining the occupancy factors of the Br atoms implies that **1** is a tetravalent or pentavalent complex cation. The molar conductivity of this complex in water gave the value of 641 $\Omega^{-1}\,\mathrm{cm}^2\,\mathrm{mol}^{-1}$. This is just between the value of 507 $\Omega^{-1}\,\mathrm{cm}^2\,\mathrm{mol}^{-1}$ for the tetravalent electrolyte, [Ni{Co(aet)$_2$(en)}$_2$]Cl$_4$,[4] and the value of 805 $\Omega^{-1}\,\mathrm{cm}^2\,\mathrm{mol}^{-1}$ for the hexavalent one, [{Rh(aet)$_3$}$_4$Zn$_4$O]Br$_6$ (**2**Br$_6$),[25] suggesting that **1** is a heptavalent complex cation. Furthermore, in the ^{1}H NMR spectrum **1** exhibits a singlet signal at δ=5.67, which has not been observed for [{Rh(aet)$_3$}$_4$Zn$_4$O]$^{6+}$ (**2**).[25] Taking these facts and the elemental analyses of the bromide and nitrate salts of **1** into consideration, it is reasonable to determine that **1** is a heptavalent complex cation with a [Zn$_3$HO]$^{5+}$ core, [{Rh(aet)$_3$}$_4$Zn$_3$HO]$^{5+}$, rather than a tetravalent complex cation with a [Zn$_3$O]$^{4+}$ core, [{Rh(aet)$_3$}$_4$Zn$_3$O]$^{4+}$.[31] That is, in **1** three Zn^{2+} coordinate to OH$^-$ to form the "defective" quasi-tetrahedral [Zn$_3$HO]$^{5+}$ core, instead of the "complete" tetrahedral [Zn$_4$O]$^{6+}$ core in **2** (Fig. 1).[19,25]

The overall structure of **1** is essentially the same as that of **2**;[19,25] the four octahedral *fac*(*S*)-[Rh(aet)$_3$] units are bound to the quasi-tetrahedral [Zn$_3$HO]$^{5+}$ core in a tetrahedral arrangement. Moreover, the bond lengths and angles in **1** are very similar to those observed in **2**.[25] However, it is noted that the Zn–O bonds in **1** (average 1.985(20) Å) are somewhat longer than those in **2** (average 1.960(17) Å), reflecting the structural difference between the [Zn$_3$HO]$^{5+}$ core and the [Zn$_4$O]$^{6+}$ one.

The complex cation **1** has two kinds of chiral centers, Δ or Λ for the *fac*(*S*)-[Rh(aet)$_3$] subunits and *R* or *S* for the bridging sulfur atoms. The absolute configurations for the spontaneously resolved $(-)^{\mathrm{CD}}_{350}$ isomer were determined by the anomalous scattering technique. The structure containing the Δ configurational *fac*(*S*)-[Rh(aet)$_3$] subunits in the complex cation is probably the correct choice and its enantiomeric structure could be rejected at the 0.005 significance level by the Hamilton test (Table 1).[32] Thus, all the *fac*(*S*)-[Rh(aet)$_3$] subunits take Δ and all the bridging sulfur atoms take *R* in $(-)^{\mathrm{CD}}_{350}$- [{Rh(aet)$_3$}$_4$Zn$_3$HO]$^{5+}$ ($(-)^{\mathrm{CD}}_{350}$-**1**), as shown in Fig. 2.

Formation. The reaction of *fac*(*S*)-[Rh(aet)$_3$] with Zn^{2+} in water under moderate conditions produced the T-cage-type S-bridged heptanuclear complex with a "defective" [Zn$_3$HO]$^{5+}$ core, [{Rh(aet)$_3$}$_4$Zn$_3$HO]$^{5+}$ (**1**). During the formation of **1**, the reaction solution turned from neutral to acidic (ca. pH=3). This suggests that the hydroxide ion incorporated into **1** comes from water, liberating the hydrogen ion in solution.

Five isomers ($\Delta\Delta\Delta\Delta$, $\Lambda\Lambda\Lambda\Lambda$, $\Delta\Delta\Delta\Lambda$, $\Lambda\Lambda\Lambda\Delta$, $\Delta\Delta\Lambda\Lambda$) are possible for **1**, considering the absolute configuration (Δ or Λ) for each of four *fac*(*S*)-[Rh(aet)$_3$] subunits. However, spontaneous resolution of **1** gave only two optical isomers, $(+)^{\mathrm{CD}}_{350}$ and $(-)^{\mathrm{CD}}_{350}$, which show CD spectra enantiomeric to each other. Furthermore, **1** was optically resolved into the $(+)^{\mathrm{CD}}_{350}$ and $(-)^{\mathrm{CD}}_{350}$

isomers with use of $[Sb_2(R,R\text{-tartrate})_2]^{2-}$ as the resolving agent. Since the $(-)^{CD}_{350}$ isomer was determined by X-ray crystallography to have the ΔΔΔΔ configuration, the $(+)^{CD}_{350}$ isomer is assignable to have the ΛΛΛΛ configuration. Thus, either of the Δ or Λ isomer of *fac*(*S*)-$[Rh(aet)_3]$ is selectively incorporated in the present $Rh^{III}_4Zn^{II}_3$ T-cage-type heptanuclear structure, $[\{Rh(aet)_3\}_4Zn_3HO]^{5+}$, forming only the ΔΔΔΔ and ΛΛΛΛ isomers with a quasi-*T* symmetry. The selective formation of the ΔΔΔΔ and ΛΛΛΛ isomers, which are spontaneously resolved, has commonly been found for the T-cage-type S-bridged octanuclear complexes with a "complete" core, $[\{M(aet)_3\}_4M'_4O]^{6+}$ (M=Co(III), Rh(III), or Ir(III); $M'_4=Zn^{II}_xCo^{II}_{4-x}$).[19,20,25]

Absorption and CD Spectra. As illustrated in Fig. 3, the absorption spectrum of yellow-orange **1** with a "defective" core is quite similar to that of yellow **2** with a "complete" core,[25] giving two d–d transition bands at ca. 27 and 31×10^3 cm^{-1} and an intense sulfur-to-rhodium charge transfer (CT) band at ca. 46×10^3 cm^{-1}, although each absorption band for **1** is broader than the corresponding band for **2**. Besides these absorption bands, **1** exhibits an absorption shoulder (ca. 24×10^3 cm^{-1}) at the lower energy side of the d–d absorption band, which is responsible for the orange-like color of **1**. This absorption shoulder is not observed for **2**, and therefore, the presence of this absorption shoulder may be taken to be diagnostic for the T-cage-type structure with a "defective" core.

Two kinds of CD contributions, one from Δ-*fac*(*S*)-$[Rh(aet)_3]$ subunits and the other from *R* configurational sulfur atoms, are expected for the ΔΔΔΔ isomer of $[\{Rh(aet)_3\}_4Zn_3HO]^{5+}$ (**1**), as in the case of ΔΔΔΔ-$[\{Rh(aet)_3\}_4Zn_4O]^{6+}$ (**2**).[19,25] As shown in Fig. 3, the CD spectral behavior of ΔΔΔΔ-**1** resembles that of ΔΔΔΔ-**2** over the whole region, giving a major negative CD band (ca. 28×10^3 cm^{-1}) in the d–d absorption band region and a negative and a positive CD bands (ca. 43×10^3 and 48×10^3 cm^{-1}) in the sulfur-to-rhodium CT band region. However, the CD intensity for **1** is much smaller than that for **2** in the sulfur-to-rhodium CT band region, while the CD intensities in the d–d band region are similar to each other. It has been recognized that for the T-cage-type S-bridged octanuclear complexes, $[\{M(aet)_3\}_4Zn_4O]^{6+}$ (M=Co(III) or Rh(III)), the bridging thiolato sulfur atoms contribute dominantly to the CD spectra in the sulfur-to-cobalt or sulfur-to-rhodium CT band region.[20,25] Therefore, the CD contribution due to the asymmetric sulfur atoms in **1** is estimated to be much smaller than that in **2**. This is compatible with the fact that nine of twelve sulfur atoms bridge the rhodium and zinc atoms to have the *R* configuration in ΔΔΔΔ-**1**, while all twelve sulfur atoms bridge the rhodium and zinc atoms in ΔΔΔΔ-**2**. Since the CD intensity in the CT band region for **1** is less than one-third for **2**, it is probable that in solution the chiral structure of the bridging sulfur atoms is not tightly fixed in **1** with a "defective" $[Zn_3HO]^{5+}$ core, in contrast to that of the bridging sulfur atoms in **2** with a "complete" $[Zn_4O]^{6+}$ core.

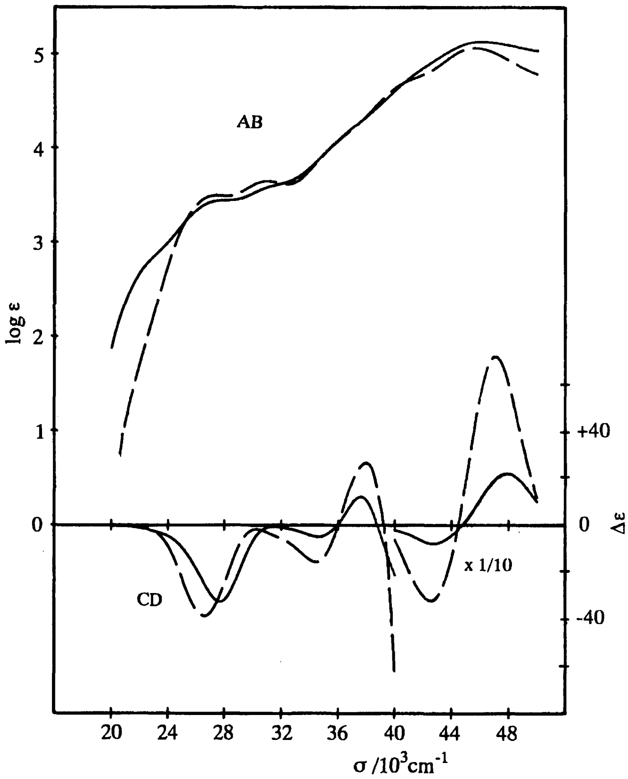

Fig. 3. Visible-UV absorption and CD spectra of ΔΔΔΔ-$[\{Rh(aet)_3\}_4Zn_3HO]^{5+}$ ($(-)^{CD}_{350}$-**1**) (—) and ΔΔΔΔ-$[\{Rh(aet)_3\}_4Zn_4O]^{6+}$ ($(-)^{CD}_{350}$-**2**) (---). ε values are given in units of $mol^{-1}\,dm^3\,cm^{-1}$.

Properties. **1** with a "defective" $[Zn_3HO]^{5+}$ core shows significant absorption and CD spectral changes with time in water especially in the sulfur-to-rhodium CT band region. This fact clearly indicates that **1** is unstable in water, dislike the T-cage-type octanuclear complexes with a "complete" $[Zn_4O]^{6+}$ core, $[\{M(aet)_3\}_4Zn_4O]^{6+}$ (M=Co(III) or Rh(III)).[19,20,25] Figure 4 shows the absorption and CD spectral changes for ΔΔΔΔ-**1** in water at room temperature. The absorption and CD spectra became approximately constant after ca. 3 h, during which time the isosbestic and isodichroic points were recognized at 215 and 219 nm, respectively. Standard first order kinetic plots of $\ln(A_\infty - A_t)$ vs. t (at 225 nm for the absorption spectral change and at 230 nm for the CD spectral change) are linear for more than 3 half-lives and from these plots the first order rate constant in water at room temperature is evaluated to be 3.2×10^{-4} s^{-1} ($t_{1/2}$=36 min). After 3 h at room temperature, the original sulfur-to-rhodium CT band at 218 nm for **1** shifts to 226 nm, of which position is consistent with that of the sulfur-to-rhodium CT band observed for the mononuclear *fac*(*S*)-$[Rh(aet)_3]$.[16,26] In the corresponding region, the CD spectrum of ΔΔΔΔ-**1**, which originally gives a negative and a positive CD

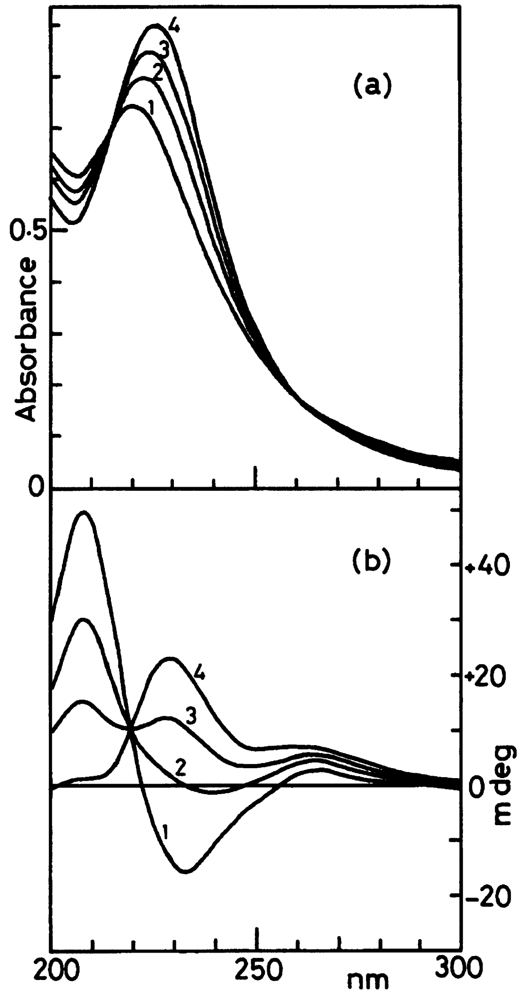

Fig. 4. Absorption (a) and CD (b) spectral changes with time in water for $\Delta\Delta\Delta\Delta$-[{Rh(aet)$_3$}$_4$Zn$_3$HO]$^{5+}$ ((−)$^{\mathrm{CD}}_{350}$-**1**); the curves 1—4 were measured at 0, 20, 60, and 180 min, respectively.

bands from longer wavelength, drastically changes to give one positive CD band at 230 nm after 3 h. This CD spectral behavior after 3 h is very similar to that of the mononuclear Δ_{LLL}-*fac*(*S*)-[Rh(L-cys-*N*,*S*)$_3$]$^{3-}$.[16] Considering these facts and the slight absorption and CD spectral changes in the d–d band region, it is suggested that the cleavage of the Zn–S bonds occurs for **1** with a "defective" core in water, retaining the coordination geometry and the absolute configuration of the *fac*(*S*)-[Rh(aet)$_3$] subunits.

Further standing the aqueous solution of **1** at room temperature resulted in the partial formation of **2** with a "complete" [Zn$_4$O]$^{6+}$ core. The formation of **2** was effectively caused by the addition of Zn^{2+} to the aqueous solution of **1** (Fig. 1). When **1** was treated with [CoCl(NH$_3$)$_5$]$^{2+}$ at 50 °C, the linear-type trinuclear complex, [Co{Rh(aet)$_3$}$_2$]$^{3+}$, was formed besides **2** (Fig. 1). This result implies that the S-bridged polynuclear structure composed of the *fac*(*S*)-[Rh(aet)$_3$] subunits is highly dependent on the metal ions incorporated in the complexes. The conversion reaction proceeds with retention of the absolute configuration of the *fac*(*S*)-[Rh(aet)$_3$] subunits, that is, $\Delta\Delta$-[Co{Rh(aet)$_3$}$_2$]$^{3+}$ and $\Delta\Delta\Delta\Delta$-**2** were formed with use of $\Delta\Delta\Delta\Delta$-**1** as the starting complex. The direct synthesis of [Co{Rh(aet)$_3$}$_2$]$^{3+}$ from *fac*(*S*)-[Rh(aet)$_3$] and [CoCl(NH$_3$)$_5$]$^{2+}$ has afforded a mixture of the $\Delta\Delta$, $\Lambda\Lambda$, and $\Delta\Lambda$ isomers,[16] and furthermore, the *fac*(*S*)-[Rh(aet)$_3$] molecule can not be optically resolved because of its sparing solubility in any solvents. Accordingly, the $\Delta\Delta\Delta\Delta$ and $\Lambda\Lambda\Lambda\Lambda$ isomers of **1**, which are selectively formed and easily optically resolved, could be available as the starting complex for the preparation of optically active S-bridged polynuclear complexes composed of the *fac*(*S*)-[Rh(aet)$_3$] subunits.

References

1) D. C. Jicha and D. H. Busch, *Inorg. Chem.*, **1**, 872 (1962).

2) D. C. Jicha and D. H. Busch, *Inorg. Chem.*, **1**, 878 (1962).

3) C. H. Wei and L. F. Dahl, *Inorg. Chem.*, **9**, 1878 (1970).

4) T. Konno, K. Okamoto, and J. Hidaka, *Inorg. Chem.*, **31**, 160 (1992).

5) D. H. Busch and D. C. Jicha, *Inorg. Chem.*, **1**, 884 (1962).

6) G. R. Brubaker and B. E. Douglas, *Inorg. Chem.*, **6**, 1562 (1967).

7) R. E. DeSimone, T. Ontko, L. Wardman, and E. L. Blinn, *Inorg. Chem.*, **14**, 1313 (1975).

8) E. L. Blinn, P. Butler, K. M. Chapman, and S. Harris, *Inorg. Chim. Acta*, **24**, 139 (1977).

9) G. R. Brubaker, M. G. Henk, and D. W. Johnson, *Inorg. Chim. Acta*, **100**, 201 (1985).

10) M. J. Heeg, E. L. Blinn, and E. Deutsch, *Inorg. Chem.*, **24**, 1118 (1985).

11) D. W. Johnson and T. R. Brewer, *Inorg. Chim. Acta*, **154**, 221 (1988).

12) T. Konno, S. Aizawa, K. Okamoto, and J. Hidaka, *Chem. Lett.*, **1985**, 1017.

13) K. Okamoto, S. Aizawa, T. Konno, H. Einaga, and J. Hidaka, *Bull. Chem. Soc. Jpn.*, **59**, 3859 (1986).

14) S. Aizawa, K. Okamoto, H. Einaga, and J. Hidaka, *Bull. Chem. Soc. Jpn.*, **61**, 1601 (1988).

15) T. Konno, S. Aizawa, and J. Hidaka, *Bull. Chem. Soc. Jpn.*, **62**, 585 (1989).

16) T. Konno, S. Aizawa, K. Okamoto, and J. Hidaka, *Bull. Chem. Soc. Jpn.*, **63**, 792 (1990).

17) T. Konno, K. Okamoto, and J. Hidaka, *Bull. Chem. Soc. Jpn.*, **63**, 3027 (1990).

18) T. Konno, K. Okamoto, and J. Hidaka, *Chem. Lett.*, **1990**, 1043.

19) T. Konno, K. Okamoto, and J. Hidaka, *Inorg. Chem.*, **30**, 2253 (1991).

20) T. Konno, T. Nagashio, K. Okamoto, and J. Hidaka, *Inorg. Chem.*, **31**, 1160 (1992).

21) K. Okamoto, T. Konno, Y. Kageyama, and J. Hidaka, *Chem. Lett.*, **1992**, 1105.

22) T. Konno, K. Okamoto, and J. Hidaka, *Inorg. Chem.*, **31**, 3875 (1992).

23) T. Konno, K. Okamoto, and J. Hidaka, *Acta Crystallogr., Sect. C*, **C49**, 222 (1993).

24) T. Konno, K. Nakamura, K. Okamoto, and J. Hidaka, *Bull. Chem. Soc. Jpn.*, **66**, 2582 (1993).

25) T. Konno, K. Okamoto, and J. Hidaka, *Inorg. Chem.*, in press.

26) M. Kita, K. Yamanari, and Y. Shimura, *Bull. Chem. Soc. Jpn.*, **56**, 3272 (1983).

27) "Enraf Nonius Structure Determination Package (SDP)," Enraf Nonius, Delft, Holland (1978).

28) G. M. Sheldrick, "SHELX76, A Program for X-Ray Crystal Structure Determination," University of Cambridge, Cambridge, U.K. (1976).

29) D. T. Cromer and J. T. Waber, "International Tables for X-Ray Crystallography," Kynoch Press, Birmingham, U.K. (1974), Vol. IV.

30) Lists of structure factors, complete bond distances and angles, and anisotropic thermal parameters are deposited as Document No. 67006 at the Office of the Editor of Bull. Chem. Soc. Jpn.

31) In a preliminary report (Ref. 18), the crystal structure of **1** has been solved by using the space group $P2_12_12_1$ and incorrectly assigned as a T-cage-type complex with a $[Zn_3O]^{4+}$ core, $[\{Rh(aet)_3\}_4Zn_3O]^{4+}$. Considering the present result, the analogous $Co^{III}{}_4Zn^{II}{}_3$ complex, which has been prepared from *fac*(*S*)-$[Co(aet)_3]$ and $ZnBr_2$ in water at room temperature, may be $[\{Co(aet)_3\}_4Zn_3HO]^{5+}$ rather than $[\{Co(aet)_3\}_4Zn_3Br]^{5+}$ (Ref. 20).

32) W. C. Hamilton, *Acta Crystallogr.*, **18**, 502 (1965).